

“Elastic fission” of very light nuclear systems

R. Cabezas, E. M. Szanto, N. Carlin, N. Added, A. A. P. Suaide, M. M. de Moura, M. Munhoz, R. Liguori Neto, J. Takahashi, R. M. dos Anjos,* W. H. Z. Cardenas, and A. Szanto de Toledo
Departamento de Física Nuclear, Instituto de Física da Universidade de São Paulo, Lab. Pelletron, Caixa Postal 66318, CEP 05315-970, São Paulo, Brazil

(Received 7 July 1999; published 28 October 1999)

The binary decay of very light nuclear systems into the ground state exit channel has been investigated for light heavy-ion collisions at energies ranging from the Coulomb barrier up to ~ 4 MeV per nucleon. A systematic analysis of 14 reactions and up to 50 angular distributions allowed the extraction of the energy thresholds (E_{ef}) for the fission channel forming the final products at the ground state (“elastic fission”). A significant suppression of the contribution of statistical processes is observed when the size of the system is reduced. This effect may be related to a relative increase of the fast and peripheral yields.
 [S0556-2813(99)03711-5]

PACS number(s): 25.70.Jj, 25.70.Gh, 25.70.Lm, 27.30.+t

In the past few years great effort has been devoted to the understanding of the reaction dynamic involving p -shell nuclei and in particular those involving weakly bound nuclei [1–6]. Systematic studies of fusion barriers in light heavy-ion reactions show an important increase in their height [7,8], leading to a suppression of the fusion process with an intensity inverse to the system size. Furthermore, as a consequence of the relatively high fission barriers predicted by the rotating liquid drop model [9] (RLDM) and the fact that for light nuclei (sd shell) the Coulomb repulsion of the protons does not overcome the nuclear attraction, the fission process has long been thought to be negligible in reactions involving light heavy-ions. Recently fission of light heavy-ion reactions has been detected [10,11], with intensities consistent with the transition state model (TSM) when realistic fission barriers are used [12]. On the other hand, because of the relatively lower average binding energy of the stable and mainly of the radioactive light nuclei, the breakup channel is expected to play a major role [4]. In order to examine the competition between all the mechanisms through which light-ion reactions may occur, we report, in this work, a systematic data analysis of elastic fission yields observed in light heavy-ion reactions accounting simultaneously and in a consistent way for the elastic, inelastic, transfer, fusion, and fission processes covering both fast direct and slow compound processes.

The experiments were performed at the University of São Paulo Pelletron Laboratory. Complete angular distributions were measured for several systems at various energies using E - ΔE particle identification. Reverse kinematics has been used for the most mass asymmetric reactions and particle-particle coincidences have been used in many cases to reduce the effect of the background in the cross section determination. The energy resolution was sufficient to separate the elastic and inelastic peaks in all cases. A complete description of the experimental setup has been presented in Refs.

[5,7]. For the completeness of the analysis, data for some reactions were taken from the literature when available [5,13,14]. The characteristic feature observed in the elastic scattering data is an oscillatory forward-peaked angular distribution with a smoothly rising yield at large angles (see Fig. 1). The most important contributions to the elastic yields were accounted for in the present work, namely, the potential shape elastic scattering, the coupling to the main inelastic channels, elastic transfer of nucleons and clusters, and finally, the contribution of statistical processes. Presently, the dynamics involving direct processes in elastic scattering is well understood and reported in the literature [15–19]. However, no consistent analysis of the elastic statistical process which may account simultaneously for the fusion and fission components exists.

In this work the shape elastic has been treated in the framework of the optical model (OM). The real potential is given by the double-folding model with a realistic density-dependent effective interaction based on the M3Y interaction [17]. The imaginary potential used to account for the loss of incident flux is given by a Woods-Saxon (WS) volume potential. The renormalization factor (N_{ei}) of the folding potential was kept within 15% of unity in most of the cases. The imaginary potential was used with a fixed geometry taken from Ref. [10].

It is important to stress that the main purpose of this work is not the extraction of unambiguous sets of OM parameters but to obtain a consistent and systematic evaluation of the yields originating from statistical processes. It is known that in the case of light heavy-ion reactions, at energies up to 2–3 times the Coulomb barrier, the fusion process carries most of the reaction flux, but near barrier energies the direct and inelastic processes become the most important processes. Therefore, it is important, in the analysis of the elastic cross section, to consider the influence of the coupling of the inelastic transitions to the elastic channel. In the present work this has been taken care of by using the coupled channel approach. The transition potential was given by the first derivative of the volume optical potential. It is known that some light-nuclei configurations may favor the elastic transfer process which is responsible, in some cases, for the rise

*Present address: Instituto de Física, Universidade Federal Fluminense, Ave. Litorânea s/n, Gragoatá, Niterói, Rio de Janeiro, Brazil.

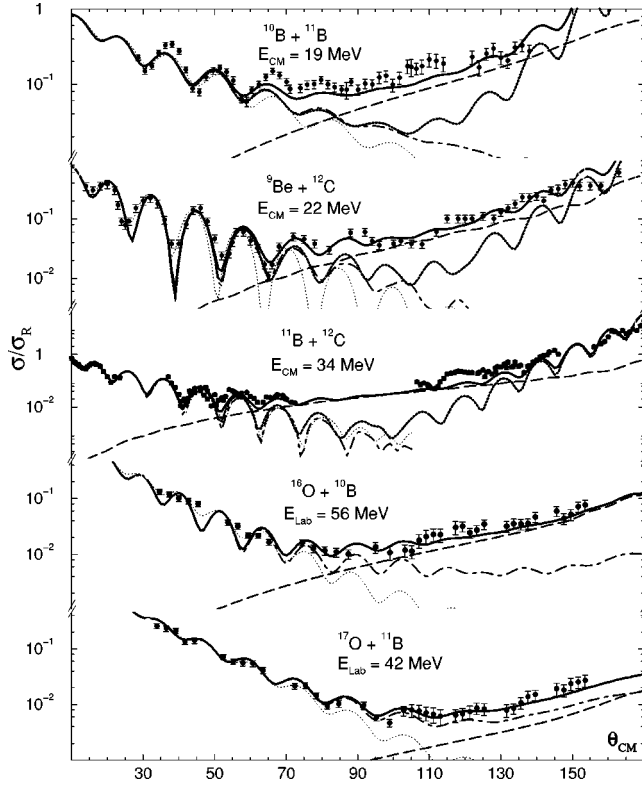


FIG. 1. Typical angular distributions for the $^9\text{Be} + ^{12}\text{C}$, $^{10}\text{B} + ^{11}\text{B}$, $^{11}\text{B} + ^{12}\text{C}$, $^{16}\text{O} + ^{13}\text{B}$, and $^{17}\text{O} + ^{11}\text{B}$ elastic channels. The curves indicate the result of the optical model calculations (dotted line), coupled channel (CC) calculations, accounting for the inelastic scattering (dash-dotted line). The inclusion of the elastic transfer (ET) amplitude to the CC, results in the thick dotted curve. The Hauser-Feshbach (HF) contribution is indicated by the dashed curves. The total elastic scattering cross section (CC+ET+HF) is described by the solid line.

of the elastic scattering cross section at back angles. Such reactions present a perfect kinematics matching and therefore are expected to occur with a significant probability when the nucleon (cluster) spectroscopic factor allows. Such contributions were evaluated within the exact finite-range (EFR) distorted wave Born approximation (DWBA) by means of the code FRESKO [19].

After the subtraction of all these direct components from the data, an angular distribution $d\sigma_{\text{elast}}/d\sigma_{\text{Rutherford}}$, with an increase at backward angles, remains, normally with a smooth nonoscillatory behavior following a $d\sigma_{\text{elast}}/d\Omega \propto 1/\sin \theta$ behavior. This remaining component has been analyzed within the statistical model framework using Hauser-Feshbach (HF) theory [21]. The continuum region of the spectrum has been described by means of the Fermi-gas level density expression [21]. Transmission coefficients for the HF calculations were consistently determined, for the elastic channel, from the coupled channel calculations of the direct components. Furthermore, the angular momentum distribution of the compound nucleus, important in the emission of heavy clusters, has been determined by the experimental cross section for the complete fusion process [4,5,7].

The fitting procedure of the data has been done in three

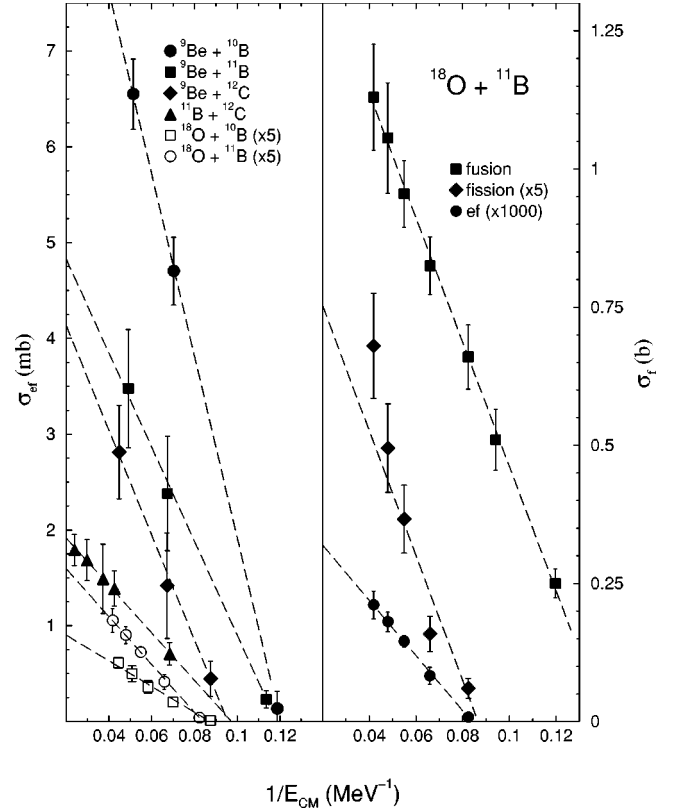


FIG. 2. Left: excitation function of the “elastic fission” yields for some systems. The dotted lines represent linear fits to the data points. Right: excitation function for the fusion [5], fission [5], and “elastic fission” yields for the $^{18}\text{O} + ^{10}\text{B}$ reaction.

steps, using the code ECIS [22]. In the first step, an optical model fit, considering only forward angle data [up to twice the grazing angle (θ_{grazing})], was performed varying two parameters, namely, the renormalization coefficient of the central folding real potential, N_{el} , and the depth of the imaginary potential, W_0 , with the geometry fixed.

In a second step, the parameters obtained in the preceding procedure are used, as starting parameters, to generate, within the coupled channel calculations, the transition potential, having at this stage three free parameters, namely, N_{el} , W_0 , and the normalization factor N_{inel} , corresponding to the transitional potential. In this step, only the first excited state of the target has been coupled to the elastic channel. χ^2 fits of the angular distributions were performed, considering the forward angles up to 3 times the grazing angle (θ_{grazing}).

In the case of systems for which the elastic transfer appeared to be relevant, namely, $\text{Be} + \text{B}$, $^{10}\text{B} + ^{11}\text{B}$, and $\text{B} + \text{C}$, this specific process has been added coherently to the shape elastic scattering using the code FRESKO [19]. Spectroscopic factors for the transferred clusters (or nucleons) were obtained from the literature [20].

In the third and last step, a simultaneous analysis is performed, using the coupled channel and Hauser-Feshbach calculations, for all the data covering the entire angular region measured. A χ^2 fit is performed adjusting four parameters N_{el} , W_0 , N_{inel} , and the normalization factor N_{HF} of the statistical model calculations. The angle-integrated value of

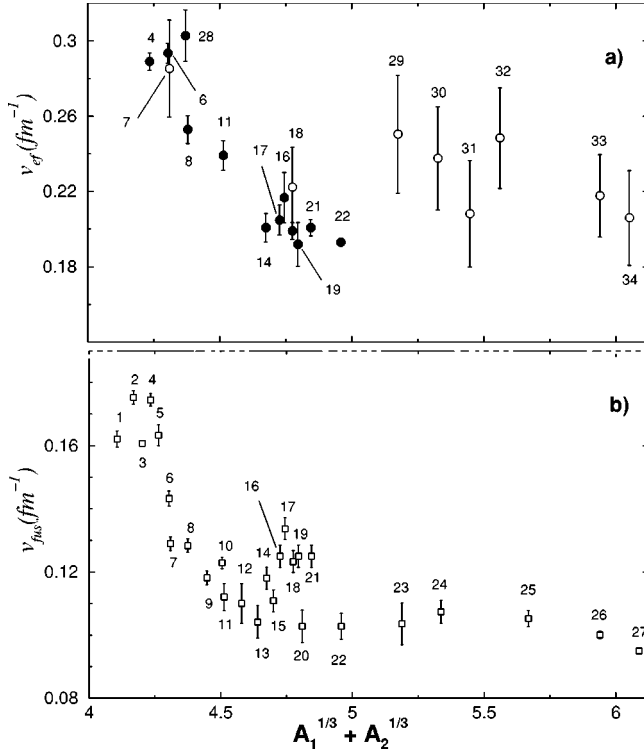


FIG. 3. Reduced values for (a) the “elastic fission” threshold v_{ef} . The open circles represent reduced fission threshold values obtained from fission cross sections and not from the elastic fission cross sections (from Ref. [14]). The dots represent the results from the present work. (b) The fusion barrier v_{fus} for light systems [5,7] as a function of the size of the system ($A_1^{1/3} + A_2^{1/3}$). The numbers represent the following systems: (1) ${}^6\text{Li} + {}^{12}\text{C}$, (2) ${}^6\text{Li} + {}^{13}\text{C}$, (3) ${}^7\text{Li} + {}^{12}\text{C}$, (4) ${}^9\text{Be} + {}^{10}\text{B}$, (5) ${}^7\text{Li} + {}^{13}\text{C}$, (6) ${}^9\text{Be} + {}^{11}\text{B}$, (7) ${}^{10}\text{B} + {}^{10}\text{B}$, (8) ${}^{10}\text{B} + {}^{11}\text{B}$, (9) ${}^{11}\text{B} + {}^{11}\text{B}$, (10) ${}^{10}\text{B} + {}^{13}\text{C}$, (11) ${}^{11}\text{B} + {}^{12}\text{C}$, (12) ${}^{12}\text{C} + {}^{12}\text{C}$, (13) ${}^{12}\text{C} + {}^{13}\text{C}$, (14) ${}^{10}\text{B} + {}^{16}\text{O}$, (15) ${}^{12}\text{C} + {}^{14}\text{N}$, (16) ${}^{11}\text{B} + {}^{16}\text{O}$, (17) ${}^{10}\text{B} + {}^{18}\text{O}$, (18) ${}^{18}\text{O} + {}^{10}\text{B}$, (19) ${}^{11}\text{B} + {}^{17}\text{O}$, (20) ${}^{12}\text{C} + {}^{16}\text{O}$, (21) ${}^{11}\text{B} + {}^{18}\text{O}$, (22) ${}^{12}\text{C} + {}^{19}\text{F}$, (23) ${}^{16}\text{O} + {}^{19}\text{F}$, (24) ${}^{19}\text{F} + {}^{19}\text{F}$, (25) ${}^{19}\text{F} + {}^{27}\text{Al}$, (26) ${}^{19}\text{F} + {}^{40}\text{Ca}$, (27) ${}^9\text{Be} + {}^{12}\text{C}$, (28) ${}^{12}\text{C} + {}^{24}\text{Mg}$, (29) ${}^{12}\text{C} + {}^{28}\text{Si}$, (30) ${}^{14}\text{N} + {}^{28}\text{Si}$, (31) ${}^{12}\text{C} + {}^{35}\text{Cl}$, (32) ${}^{16}\text{O} + {}^{40}\text{Ca}$, and (33) ${}^{35}\text{Cl} + {}^{62}\text{Ni}$.

this statistical component is taken as the “elastic fission” cross section.

Typical fits to the angular distributions are presented in Fig. 1 together with the partial contributions of the processes considered. The excitation function of the “elastic fission” cross section increases rapidly with energy for all the systems investigated and display a quasilinear dependence on $1/E_{c.m.}$ similar to the complete fusion cross section. This behavior is consistent with the interpretation of a statistical component describing the back angle elastic yields. Fits of the excitation functions to the Glas-Mosel model [5,7] allow the extraction of values for the “elastic fission” threshold (E_{ef}) which correspond to the intersection of the curve with the $1/E_{c.m.}$ axis (see Fig. 2). The “elastic fission” threshold is related to the fission barrier of the system, the compound nucleus Coulomb parameter, the Coulomb barrier $V_{cb} = Z_1 Z_2 e^2 / r_0 (A_1^{1/3} + A_2^{1/3})$, and its rotational energy. Because of the fact that at the threshold energy the angular momen-

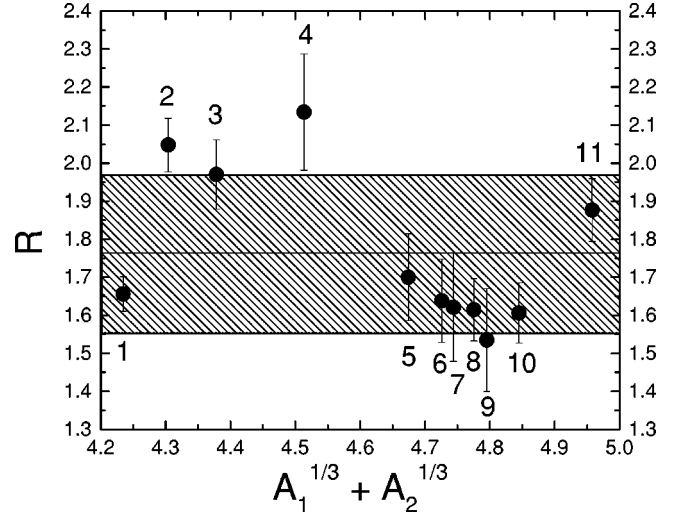


FIG. 4. Ratio between the reduced values of the “elastic fission” and the fusion barriers, $R = v_{ef} / v_{fus}$, for the systems investigated in the present work as a function of the size of the system $A_1^{1/3} + A_2^{1/3}$. The hatched lines represent the average value for R and their width represents its uncertainty. The numbers represent the following systems: (1) ${}^9\text{Be} + {}^{10}\text{B}$, (2) ${}^9\text{Be} + {}^{11}\text{B}$, (3) ${}^{10}\text{B} + {}^{11}\text{B}$, (4) ${}^{11}\text{B} + {}^{12}\text{C}$, (5) ${}^{16}\text{O} + {}^{10}\text{B}$, (6) ${}^{17}\text{O} + {}^{10}\text{B}$, (7) ${}^{16}\text{O} + {}^{11}\text{B}$, (8) ${}^{18}\text{O} + {}^{10}\text{B}$, (9) ${}^{17}\text{O} + {}^{11}\text{B}$, (10) ${}^{18}\text{O} + {}^{11}\text{B}$, and (11) ${}^{19}\text{F} + {}^{12}\text{C}$.

tum is relatively low, we expect that the value of E_{ef} should be closely related to the elastic fission barrier.

Explicit expressions for the appropriate fission widths for light systems can be found in Ref. [11] and are based on the Sierk [9] fission barriers. Saddle configurations in light systems are believed to have the shape of two touching spheroids separated by a very small neck. Therefore, the scission point is expected to be, in shape and energetically, very close to the saddle configuration. In the specific case of the “elastic fission” where fragments are at the lowest temperature and smallest deformation, the transmission coefficients for the entrance and exit channels are identical. The fission branching ratio is determined by the phase space at the saddle point. However, in the case of light systems for which the saddle and scission points are practically equivalent, this phase space is comparable to the number of open channels in the final fragments. Consequently, the predictions from the transition state model which has been successful in the description of the fission process of light heavy-ion reactions [11] are equivalent to those given by Hauser-Feshbach theory. Support for this assumption is given by the fact that the total kinetic energy (TKE) of the strongly damped fragments is very closely related to the sum of the relative nuclear, Coulomb, and rotational energies of two spheroids [5]. It is interesting to note [see Fig. 2(b)] that the fusion, fission, and “elastic fission” excitation functions have similar behavior. However, different barrier values are obtained due to the different phase spaces available to the different exit channels.

Reduced values for the energy thresholds for the “elastic fission” channels $v_{ef} = E_{ef} / Z_1 Z_2 e^2$ are presented in Fig. 3(a) and the reduced fusion barrier v_{fus} (extracted from evaporation residues cross sections [7]) are presented in Fig. 3(b). A

systematic increase of v_{fus} for systems forming compound nuclei lighter than $A_{\text{cn}} < 30$ is clearly observed, leading to an inhibition of the complete fusion process for those light nuclei. It is interesting to note that the value for the reduced “elastic fission” energy threshold v_{ef} shows a similar behavior and an equivalent reduction for systems of the same size, indicating that both processes are associated with statistical processes and both are suppressed for very light systems. It is important to remember that the formation of an equilibrated compound nucleus (complete fusion) is associated with an entrance channel effect whereas the “elastic fission” process is sensitive to the entrance and exit channels.

Figure 3 indicates that the onset of the hindrance of the statistical processes (fusion, fission, and “elastic fission”) occurs at the same mass region ($A_1^{1/3} + A_2^{1/3} < 4.7$). The enhancements of the barriers v_{ef} and v_{fus} are of similar intensity. This fact can be clearly seen when we calculate the ratio $R = v_{\text{ef}}/v_{\text{fus}}$ as a function of the size of the system, as shown in Fig. 4. The ratio R presents a constant behavior over the entire mass region investigated. This onset mass $A_1^{1/3} + A_2^{1/3} < 4.7$ can be related to the atomic number of nuclei for which the nuclear density distributions no longer present the volume saturation (core or Fermi type density distribution) and are dominated by a nuclear skin (surface). As a conse-

quence, the binding energy per nucleon is below the average saturation value of 8 MeV/nucleon. In this case, the extension of the surface becomes relevant in determining the importance of the direct processes, associated with peripheral collisions.

In conclusion, we have shown that the presence of “elastic fission” processes in light heavy-ion reactions has been clearly identified. The data presented in this paper also show that, as we go to lighter ions, statistical processes become relatively inhibited. Although it is established that at barrier energies the coupling of collective degrees of freedom contributes to the enhancement of the fusion cross section, it has also been shown that the breakup process inhibits fusion [3,4]. We can also conclude from the present work that the correlation established between the separation energy of the colliding nuclei and the fusion probability [4] includes, besides the intrinsic effect of the binding energy, a geometrical effect scaled by the size of the system, when light nuclei are involved.

This work was supported by the Conselho Nacional de Desenvolvimento Científico e Tecnológico (CNPq), Brazil and Fundação de Amparo à Pesquisa do Estado de São Paulo- SP, Brazil.

-
- [1] S.J. Sanders, A. Szanto de Toledo, and C. Beck, *Phys. Rep.* **311**, 487 (1999).
 [2] C. Signorini, *J. Phys. G* **23**, 1235 (1997).
 [3] J.J. Kolata *et al.*, *Phys. Rev. C* **57**, R6 (1998).
 [4] J. Takahashi, M. Munhoz, E.M. Szanto, N. Carlin, N. Added, A.A.P. Suaide, M.M. Moura, R. Liguori Neto, A. Szanto de Toledo, and L.F. Canto, *Phys. Rev. Lett.* **78**, 30 (1997).
 [5] R.M. Anjos, N. Added, N. Carlin, L. Fante, Jr., M.C.S. Figueira, R. Matheus, E.M. Szanto, C. Tenreiro, A. Szanto de Toledo, and S.J. Sanders, *Phys. Rev. C* **49**, 2018 (1994).
 [6] S.J. Sanders, *Phys. Rev. C* **44**, 2676 (1991).
 [7] L. Fante, Jr., N. Added, R.M. Anjos, N. Carlin, M.M. Coimbra, M.C.S. Figueira, R. Matheus, E.M. Szanto, and A. Szanto de Toledo, *Nucl. Phys.* **A552**, 82 (1993).
 [8] C. Beck, Y. Abe, N. Aissaoui, B. Djerroud, and F. Haas, *Phys. Rev. C* **49**, 2618 (1994).
 [9] A.J. Sierk, *Phys. Rev. C* **33**, 2039 (1986).
 [10] R.M. Anjos, N. Added, N. Carlin, L. Fante, Jr., M.C.S. Figueira, R. Matheus, H. Schelin, E.M. Szanto, C. Tenreiro, and A. Szanto de Toledo, *Phys. Rev. C* **48**, R2154 (1993).
 [11] S.J. Sanders, *Phys. Rev. C* **49**, 1016 (1994).
 [12] K.A. Farrar *et al.*, *Phys. Rev. C* **54**, 1249 (1996).
 [13] S. Albergo *et al.*, *Phys. Rev. C* **43**, 2704 (1991).
 [14] C. Beck and A. Szanto de Toledo, *Phys. Rev. C* **53**, 1989 (1996).
 [15] D.T. Khoa, G.R. Satchler, and W. von Oertzen, *Phys. Lett. B* **358**, 14 (1995).
 [16] D.T. Khoa, W. von Oertzen, and H.G. Bohlen, *Phys. Rev. C* **49**, 1652 (1994).
 [17] G.R. Satchler, *Nucl. Phys.* **A279**, 493 (1977).
 [18] A.M. Kobos, B.A. Brown, P.E. Hodgson, G.R. Satchler, and A. Budzanowski, *Nucl. Phys.* **A384**, 65 (1982).
 [19] J.J. Thompson, *Comput. Phys. Rep.* **7**, 167 (1988).
 [20] E. Kwasniewicz and J. Kisiel, *J. Phys. G* **13**, 121 (1987).
 [21] R.G. Stokstad, in *Treatise on Heavy-Ion Science*, edited by D.A. Bromley (Plenum, New York, 1985).
 [22] J. Reynal, computer code, ECIS88 (unpublished).